OrtR regulates the oxidative stress response of *Streptococcus mutans*

Shuxing Yu[1, 2], Jun Huang[1, 2], Yaqi Liu[1, 2], Jing Li[1, 2], Qiong Zhang[1, 2], Yan Wang[1, 2], Tao Gong[1], Qizhao Ma[1, 2*], Jing Zou[1, 2*], Yuqing Li[1*]

[1] State Key Laboratory of Oral Diseases, National Clinical Research Center for Oral Diseases, West China Hospital of Stomatology, Sichuan University, Chengdu, China

[2] Department of Pediatric Dentistry, West China Hospital of Stomatology, Sichuan University, Chengdu, China

Running title: OrtR and oxidative stress response

* Correspondence authors

Email: mqz2080@163.com (QM); zoujing@scu.edu.cn (JZ); liyuqing@scu.edu.cn (YL)

*These authors contributed equally to this work.

Abstract

Dental caries is the most common chronic infectious diseases around the world and disproportionately affects the marginalized socioeconomic group. *Streptococcus mutans*, considered a primary etiological agent of caries, must depend on the coordinated physiological response to tolerate the oxidative stress generated by commensal species within dental plaque, which is a critical aspect of its pathogenicity. Here, we identified and characterized a novel TetR family regulator named OrtR (oxidative stress adaptation-related transcriptional regulator), encoded by the TnSmu2 operon, which appears to be acquired by the bacteria via horizontal genes transfer. Surprisingly, *ortR* functions as a transcriptional repressor to regulate gene expression outside its operon, involved in the oxidative stress response of *S. mutans*. The *ortR* overexpression strain UA159/pDL278-*ortR* was more susceptible to oxidative stress and less competitive against hydrogen peroxide generated by commensal species *Streptococcus gordonii* and *Streptococcus sanguinis*. Transcriptomics analysis revealed that *ortR* overexpression resulted in the significant downregulation of 22 genes mainly belonging to three gene clusters responsible for the oxidative stress response. The conversed DNA binding motif of OrtR was determined by electrophoretic mobility shift and DNase I footprinting assay with purified OrtR protein, therefore, *ortR* is directly involved in gene transcription related to the oxidative stress response. Crucially, our finding provides a new understanding of how *S. mutans* deals with the oxidative stress that is required for pathogenesis and will facilitate the development of new and improved therapeutic approaches for dental caries.

Keywords: dental caries, biofilm, hydrogen peroxide, transcription factor, transcriptome, gene expression

Author summary

Streptococcus mutans is the major organism associated with the development of dental caries, which globally is the most common chronic disease. To persist and survive in biofilms, *S. mutans* must compete with commensal species which occupy the same ecological niche. Here, we uncover a novel molecular mechanism of how TetR family regulator *ortR* encoded by the TnSmu2 genomic island involves in the oxidative stress response through transcriptomics analysis, electrophoretic mobility shift assay, and DNase I footprinting assay. Furthermore, we demonstrated that *ortR* mediates *S. mutans* sensitivity to oxidative stress and competitiveness with commensal streptococci. Therefore, this study has revealed a previously unknown regulation between *ortR* and genes outer its operon and demonstrated the importance of *ortR* in the oxidative stress response and the fitness of S. mutans within the plaque biofilms, which can be exploited as a new therapy to modulate the ecological homeostasis and prevent dental caries.

Introduction

Dental caries, characterized by the demineralization and subsequent destruction of teeth, is the most prevalent biofilm-associated oral infectious disease globally [1,2]. The

63 pathogenesis of dental caries is considered to be a microbial shift in the biofilm
64 composition; however, *Streptococcus mutans* is the most closely and constantly linked with
65 caries formation [3,4]. Occasionally, *S. mutans* can enter the bloodstream and cause
66 systemic infections, such as infective endocarditis [5–7].

67 *S. mutans* resides in biofilms on the tooth surface, which is a diverse, multi-species,
68 and dynamic environment that is constantly exposed to severe limitations in nutrition,
69 fluctuations in temperature and pH, and challenges in osmotic and oxidative tensions [8,9].
70 To survive adverse environmental conditions, bacteria evolve through a wide range of rapid
71 and adaptive responses, including carbohydrate utilization, acid production, and low pH
72 adaption, which are well-studied [10,11]. However, limited information is available
73 regarding oxidative stress response and its impact on the adaptation of *S. mutans*. In a
74 previous transcriptomic study that measured gene transcripts expressed in natural oral
75 biofilm communities, the majority of stress response transcripts (50%–75% of total) were
76 associated with oxidative stress, suggesting that oxidative stress is the leading stressor in
77 the biofilm microbial communities [12,13].

78 Multiple sources contribute to oxidative stress, including the poisonous effects of
79 reactive oxygen species (ROS) and unfavorable cellular redox potential [14,15]. Damaging
80 ROS, including superoxide anion radical ($O2^{\cdot-}$), hydrogen peroxide (H_2O_2), and hydroxyl
81 radical ($HO\cdot$), are produced inside the bacterial cells when growing in an aerobic
82 environment. $O2^{\cdot-}$ and $HO\cdot$ derives from Fenton chemistry as part of the bacterial oxidative
83 stress pathway [16,17]. ROS are toxic and can react more voluntarily with biological

84 macromolecules, such as cleaving RNA/DNA, and oxidizing proteins and lipids [18,19].
85 Therefore, the ability of *S. mutans* to cope with oxidative stress is important for their
86 survival and perseverance in dental biofilm microbial communities.

87 In RNA sequencing (RNA-Seq) analysis, evidence for oxidative stress tolerance is
88 revealed in a large genomic island termed TnSmu2 [20]. Many genes encoded within the
89 TnSmu2 regions are affected in the deletion of *fstH*, *cidB,* or *covR*, which are involved in
90 oxidative stress resistance [21–23]. TnSmu2 is a mobile genetic element commonly
91 acquired through horizontal gene transfer events, which is a selective competitive growth
92 advantage seen under changing environmental conditions that affects the metabolism or
93 pathogenic potential of the organisms [24–26]. The region contains two tetracycline
94 repressor (TetR) family transcriptional regulators, *smu_1349* and *smu_1361c* [27,28].
95 *smu_1349* is involved in oxidative stress response by regulating the nonribosomal peptide
96 synthetase-polyketide synthase gene cluster [28]. However, the regulatory effect of
97 *smu_1361c* on the oxidative stress tolerance of *S. mutans* is still uncharacterized. Therefore,
98 we suggest a hypothesis that *smu_1361c*, carried on the TnSmu2 genomic island, provides
99 an additional layer of the regulatory mechanism of oxidative stress for *S. mutans*.

100 Herein, we investigated the function of the transcription factor SMU_1361c, renamed
101 OrtR (oxidative stress adaptation-related transcriptional regulator), and uncovered its
102 regulatory mechanism on the oxidative stress response. OrtR inhibits the gene expressions
103 of *smu_137-141* and *smu_764-765* by directly binding to their promoters, attributing to the
104 observed defects of *S. mutans* in tolerance against oxidative stress. This study highlights a

105 new link between OrtR from the TnSmu2 regions and the oxidative stress response and
106 provides a new possible goal for the ecological control of dental caries.
107

108 Results

109 OrtR increased susceptibility to the oxidative stress response of 110 *S. mutans*

111 The overexpression and in-frame deletion mutants for *ortR* were constructed to evaluate
112 the function of OrtR. First, we measured the mRNA levels of *ortR* in UA159,
113 UA159/pDL278, UA159/pDL278-*ortR*, and UA159 Δ*ortR*, using quantitative reverse
114 transcription polymerase chain reaction (qRT-PCR). As shown in S1 Fig, the expression
115 level of *ortR* in the strain overexpression *ortR* increased significantly, about 50-fold,
116 compared with that of UA159/pDL278, and no *ortR* transcripts were detected in the *ortR*
117 deletion strain, as expected. These results indicate that both the *ortR* in-frame deletion
118 mutants for *ortR* were successfully constructed.

119 We first measured the growth rates of UA159, UA159/pDL278, UA159/pDL278-*ortR*,
120 and UA159 Δ*ortR* under aerobic conditions. As shown in Fig 1A, no significant differences
121 were observed between these bacterial growths both in the logarithmic growth and
122 stationary phase. Since the ability to form biofilm is an important virulence factor in *S.*
123 *mutans*, the effect of *ortR* on biofilm formation at different times (6, 12, and 24 h) was
124 examined. Similarly, no significant differences were observed in biofilm biomass (Fig 1B).

125 Furthermore, the effect of *ortR* on other key virulence properties and bacterial fitness
126 was detected. The study results showed that there were no significant differences in
127 acidogenicity and aciduricity of the UA159, UA159/pDL278, UA159/pDL278-*ortR*, and
128 UA159 Δ*ortR* strains (S2A and 2B Fig). To compare their ability to grow and survive when
129 exposed to hydrogen peroxide, a hydrogen peroxide killing assay was performed, where
130 the percent viable cells were determined after exposure to hydrogen peroxide for 20, 40,
131 and 60 min. After 20 min of exposure to hydrogen peroxide, the overexpression strain
132 UA159/pDL278-*ortR* showed a slight defect in the ability to survive (Fig 1C and 1D).
133 However, after 40 or 60 min of exposure, there was a significant decrease in the ability of
134 the UA159/pDL278-*ortR* strain to survive, with no significant differences observed for
135 UA159 Δ*ortR* compared with the UA159/pDL278 strain and *S. mutans* UA159 (Fig 1C
136 and 1D). This result was further supported by the findings in Fig 1E and 1F. A dose-
137 dependent inhibition was observed when filter disks infused with different hydrogen
138 peroxide concentrations ranging from 20 to 60 mM were placed on a soft agar plate
139 containing UA159 and its derivatives, particularly in the overexpression strain
140 UA159/pDL278-*ortR*. Together, these results suggest that *ortR* plays an important role in
141 oxidative stress response in *S. mutans*.
142

143 OrtR impaired bacterial competitiveness of *S. mutans* in the 144 three-species biofilms

145 The tooth surfaces are colonized by a great number of bacterial species, which normally
146 maintain ecological homeostasis amid different species. Hydrogen peroxide-producing
147 commensal species, including *Streptococcus gordonii* and *Streptococcus sanguinis*, are
148 among many of the early colonizers on tooth surfaces [29,30]. Therefore, the ability of *S.*
149 *mutans* to contend with oxidative stress generated by hydrogen peroxide is important for
150 its competitiveness with commensal species that occupy the same ecological niche [31–
151 33]. Subsequently, we probed the potential function of *ortR* in regulating the
152 competitiveness of *S. mutans* in oral biofilm communities by creating a three-species
153 biofilms model, comprising *S. mutans*, *S. sanguinis*, and *S. gordonii*. Fluorescent in situ
154 hybridization (FISH) was used to visualize the spatiotemporal interactions within the three-
155 species biofilm communities (Fig 2A). Quantitative analysis of FISH-labeled biofilms
156 showed that the overexpression strain UA159/pDL278-*ortR* was less competitive than the
157 UA159/pDL278 strain against *S. sanguinis* and *S. gordonii* (Fig 2B). No significant
158 competitiveness differences were observed between UA159 and UA159 Δ*ortR* (Fig 2B).
159 To determine whether the less competitiveness of UA159/pDL278-*ortR* is caused by
160 hydrogen peroxide produced by *S. sanguinis* and *S. gordonii*, we detected the effect of
161 hydrogen peroxide on bacterial interactions by adding catalase to the three-species biofilms.
162 As shown in Fig 2C and 2D, there was a superior competitive advantage of
163 UA159/pDL278-*ortR* against *S. sanguinis* and *S. gordonii* over UA159/pDL278; no
164 significant competitive differences were observed between UA159 and UA159 Δ*ortR*
165 against *S. sanguinis* and *S. gordonii*, within three-species biofilms (Fig 2C and 2D). These

166 results indicated that *ortR* impairs the competitiveness of *S. mutans* in biofilm communities
167 owing to the sensitivity to hydrogen peroxide produced by commensal *S. gordonii* and *S.*
168 *sanguinis*.
169

170 Transcriptomics analysis of the UA159/pDL278-*ortR* strain

171 To understand the role *ortR* plays globally in regulating oxidative stress response of *S.*
172 *mutans*, transcriptomics analysis of the UA159/pDL278 and UA159/pDL278-*ortR* strains
173 was performed. In total, 22 significantly downregulated genes (>2-fold) and 14
174 significantly upregulated genes (>2-fold) were identified in the UA159/pDL278-*ortR*
175 strain compared with UA159 (Fig 3A, S3 and S4 Tables). Among the up-regulated genes
176 in this range was the gene *ortR*, which further supported the previous qRT-PCR results
177 (S1A Fig). Based on the *S. mutans* UA159 genome annotation from the National Center
178 for Biotechnology Information, most of the significantly downregulated genes were mainly
179 associated with energy production and conversion and carbohydrate transport and
180 metabolism, except for some unannotated genes (Fig 3A). The volcano plot illustrates
181 considerably downregulated gene clusters, including *smu_137-smu_141*, *smu_764-*
182 *smu_765*, and *smu_127-smu_130*, and the highest upregulated gene *smu_1361c* (*ortR*) in
183 the UA159/pDL278-*ortR* strain compared with UA159/pDL278 strain (Fig 3B).
184 To better condense the differentially expressed genes (DEGs) into functional gene
185 groups, the DAVID bioinformatic tool (https://david.ncifcrf.gov/) was used to conduct the
186 Kyoto Encyclopedia of Genes and Genomes (KEGG) pathway and Gene Ontology (GO)

187 enrichment analysis [34,35]. DEGs were enriched in six KEGG pathways and six GO terms
188 (Fig 3C and 3D). The KEGG pathway enrichment analysis showed that the downregulated
189 genes belonged to the citrate cycle (tricarboxylic acid cycle), pyruvate metabolism,
190 glycolysis/gluconeogenesis, carbon metabolism, microbial metabolism, microbial
191 metabolism in diverse environments, and biosynthesis of secondary metabolites (Fig 3C,
192 S3 and S5 Tables). The GO enrichment analysis showed that the downregulated genes were
193 mainly involved in peroxidase activity, peroxiredoxin activity, transferase activity, cell
194 redox homeostasis, flavin adenine dinucleotide binding, and sugar phosphotransferase
195 activity (Fig 3D, S3 and S6 Tables).

196 Among these DEGs, *mleS* (*smu_137*) for a malolactic enzyme, *mleP* (*smu_138*) for
197 malate permease, *gshR* (*smu_140*) for a glutathione reductase, *ahpC* (*smu_764*) for an alkyl
198 hydroperoxide reductase, and *smu_765* for the NADH oxidase/alkyl hydroperoxidase
199 reductase peroxide-forming known to associate with the oxidative stress response of *S.*
200 *mutans* were significantly downregulated in the UA159/pDL278-*ortR* strain compared
201 with those in UA159/pDL278. In addition, the gene cluster *smu_127-smu_130* was
202 significantly downregulated in UA159/pDL278-*ortR*, which was also recently reported to
203 be involved in the oxidative stress response of *S. mutans* [36]. Significantly, these results
204 indicate that *ortR* may regulate their gene expression by affecting the promoter of these
205 gene clusters (Fig 3B and 3E).

206

207 **OrtR directly bound to the promoters of *smu_137-smu_141* and**
208 ***smu_764-smu_765***

209 Based on the phenotype results that the UA159/pDL278-*ortR* strain was more sensitive to
210 oxidative stress than the UA159/pDL278 strain, the promoters of *smu_137-smu_141* and
211 *smu_764-smu_765* were chosen to study the DNA binding activity and specificity of OrtR
212 and were renamed *smu_137* promoter and *smu_764* promoter in subsequent studies,
213 respectively. The *smu_137* promoter (116 bp) and *smu_764* promoter (131 bp) were
214 amplified to investigate their interactions with purified recombinant His-OrtR protein using
215 EMSA, and the *smu_136c* ORF fragment (116 bp) and *smu_765* ORF fragment (131 bp)
216 were used to exclude the nonspecific bindings of OrtR to DNA substrates (Fig 4A and 4B).
217 The mobility shifts were only observed when OrtR was incubated with the *smu_140*
218 promoter and *smu_764* promoter, and no mobility shifts appeared when OrtR was
219 incubated with the *smu_136c* ORF fragment and 131 bp *smu_765* ORF fragment (Fig 4A
220 and 4B). These results indicate that OrtR can directly bind to the promoters of *smu_137-*
221 *smu_141* and *smu_764-smu_765*.

222

223 **Identifying the specific binding motif of OrtR**

224 The DNase I footprinting assay was used to demonstrate the specific binding motif of OrtR
225 to the putative *smu_137* promoter region. After the *smu_137* promoter region was exposed
226 to DNase I, the fragment containing 5′-CATATTATAACATAAAATG-3′ with high AT
227 content was gradually protected with the increasing OrtR concentrations (Fig 5A). To

228 further confirm that this motif was essential for the OrtR recognition, two DNA substrates,
229 *smu_137* promoter 1 (p1) containing 5′-CATATTATAACATAAAATG-3′ and *smu_137*
230 p1mut (A and T bases were changed to C and G in the palindrome sequence, respectively)
231 containing 5′-CCGCGGCGCCCCGCCCCGG-3′ were designed and amplified (Fig 5B).
232 The EMSA results showed that OrtR formed the protein/DNA complex with *smu_137* p1
233 (Fig 5B). No complex/DNA complex with *smu-137* p1mut were formed obviously (Fig
234 5B). These results indicate that the DNA motif 5′-CATATTATAACATAAAATG-3′ is the
235 binding site recognized by OrtR. The putative OrtR binding motif in other promoters was
236 searched using MEME Suite 5.5.1. Then, another two putative OrtR binding sequences
237 were found in the *smu_764* promoter (5′-ATTATAAGAAAA-3′) and *smu_127* promoter
238 (5′-ATTTTAACATAA-3′), in which the repressing regulation of OrtR accounts for the
239 downregulated genes in the transcriptomics analysis (Fig 4C). A further logo assay was
240 performed using WebLogo tool (University of California, Berkeley) (Fig 5C).
241

242 # Disscussion

243 Oral biofilms are microbial communities with a high density and diversity of bacterial
244 species; these species both cooperate and compete with one another [37,38]. Many
245 commensal bacteria, such as *S. gordonii* and *S. sanguinis*, are the initial colonizers on the
246 tooth surface before *S. mutans* [39,40]. They create oxidative stress conditions by
247 producing hydrogen peroxide, which gives them the ability to compete with *S. mutans* for
248 the same ecological niche [41,42]. Therefore, the ability to tolerate oxidative stress is vital

249 for the survival and fitness of *S. mutans* in oral biofilms. Our study results reveal that OrtR,
250 a novel TetR transcription factor, impairs the oxidative stress response by regulating the
251 expression of multiple related virulence genes in *S. mutans* and further provide insights
252 into the molecular mechanisms of OrtR as a transcription repressor that manipulates
253 numerous related virulence genes in *S. mutans* by directly binding to their specific
254 promoter regions.

255 Since *S. mutans* lacks catalase, alternative strategies must be used to cope with the
256 oxidative stress challenges imposed by the competing species and host [43,44]. In this
257 study, we found that the overexpression strain UA159/pDL278-*ortR* was more sensitive to
258 hydrogen peroxide stress than the UA159/pDL278 strain (Fig 1C–F). In addition, the *ortR*
259 overexpression decreased the ability of *S. mutans* to compete with *S. gordonii* and *S.*
260 *sanguinis* in the well-characterized interspecies interaction three-species biofilms model,
261 signifying that the ability to tolerate oxidative stress is impaired (Fig 2A and 2B). This
262 inhibition phenotype was lost when catalase was added to the three-species biofilms,
263 further approving that this inhibition of overexpression strain UA159/pDL278-*ortR* was a
264 function of hydrogen peroxide generated by *S. gordonii* and *S. sanguinis*. These phenotypes
265 were consistent with the transcriptomics analysis results of UA159/pDL278 and
266 UA159/pDL278-*ortR*. For example, the downregulated gene clusters including *smu_137-*
267 *smu_141*, *smu_764-smu_765*, and *smu_127-smu_130* are closely associated with the
268 oxidative adaptive adaptability of *S. mutans* , which attribute to the observed defects of
269 UA159/pDL278-*ortR* in tolerance against hydrogen peroxide (Fig 3B and 3E).

270 The TetR family, a family of transcriptional regulators, is well represented and widely
271 distributed amid bacteria with a DNA-binding motif, whose function is usually that of
272 repressors [45,46]. In this study, the expression levels of the three operons associated with
273 the oxidative stress response were downregulated when the *ortR* gene was overexpressed,
274 confirming that OrtR acts as a repressor of operon expression, as seen as in other family
275 members of *S. mutans*, such as *mubR*, *hapR*, *accR* and *frtR* [34,47–49]. In detail, the
276 deletion of *mubR* and *frtR* downregulated the transcription of NRPS-PKS gene clusters and
277 *frtP* gene, which are responsible for amplified sensitivity to oxidative stress and fluoride,
278 respectively. Furthermore, the GO terms for the downregulated genes were compared, and
279 several genes related to phosphotransferase system, the major route for internalization of
280 carbohydrates in *S. mutans*, were differentially downregulated in the overexpression strain
281 UA159/pDL278-*ortR* (Fig 3D). *ortR* may fine-tune cellular physiology during periods of
282 oxidative stress to help preserve normal cellular homeostasis.

283 According to the transcriptomics analysis in this study, *ortR* does not show a
284 regulatory relationship with its neighboring genes; however, it is involved in the regulation
285 of genes outside its operon. The EMSA results support a direct mechanism for the OrtR
286 regulation of two gene clusters *smu_137*-*smu_141* and *smu_764*-smu_*765*. The binding
287 motif was identified by DNase I footprinting assays, and the results showed that a
288 palindromic sequence with high AT content was protected by OrtR, suggesting that OrtR
289 prefers binding to DNA motif with high AT content. The preference was consistent with
290 other TetR family transcription factors, such as MubR, HapR, AccR or FrtR [34,47–49].

291 In summary, OrtR, a novel TetR family transcription factor, acts as a repressor to
292 impair the ability of *S. mutans* to survive and compete with commensal bacteria due to the
293 sensitivity to their by-product, hydrogen peroxide. Further studies have explained that *ortR*
294 leads to significant reductions in several gene clusters involved in the oxidative stress
295 response by binding to their specific promoter regions. Thus, an improved understanding
296 of the mechanism by which OrtR regulates the *S. mutans* oxidative stress response can
297 strengthen our understanding to exploit interspecies interactions in the plaque biofilm for
298 reducing dysbiosis-induced cariogenesis.
299

300 Materials and Methods

301 Bacterial strains and growth conditions

302 All strains, plasmids, and primers used in this study are listed in the S1 and S2 Tables. *S.*
303 *mutans* UA159, *S. gordonii* DL1, and S. sanguinis SK36 were obtained from the State Key
304 Laboratory of Oral Diseases (Sichuan University, Chengdu, China). *S. mutans* UA159 and
305 its derivatives, *S. gordonii* DL1, and *S. sanguinis* SK36 were routinely grown in brain heart
306 infusion (BHI) broth (Difco, Sparks, MD, United States) or on BHI agar incubated
307 aerobically for 24 h at 37 °C. For the biofilm formation assay, 1% sucrose (wt/vol, Sigma,
308 United States) was added to the BHI medium (BHIS). In addition, *Escherichia coli* and its
309 derivatives were cultured in Luria-Bertani medium (BD, Sparks, MD, United States)
310 aerobically (95% air, 5% CO_2) with spectinomycin (1 mg/mL) or kanamycin (30 μg/mL)
311 at 37°C, when necessary.

312

313 Construction of overexpression strains

314 The genes of ortR and *ldh* promoter regions were amplified from *S. mutans* genomic DNA
315 by polymerase chain reaction (PCR). All the primers were designed using an online tool
316 provided by TaKaRa (https://www.takarabio.com/learning-centers/cloning/primer-design-
317 and-other-tools) and listed in S2 Table. The PCR products were purified and cloned into
318 linearized *E. coli*-*Streptococcus* shuttle vector pDL278 by using an In-Fusion HD cloning
319 kit (TaKaRa, Japan) as described previously [50]. Then, the recombined plasmid was
320 transformed into *S. mutans* UA159 to generate overexpression strains UA159/pDL278-
321 *ortR*, which were selected by using plates containing spectinomycin (1 mg/mL) and
322 verified by PCR and sequencing.

323

324 Construction of markerless in-frame deletion strains

325 The markerless in-frame deletion strain UA159 Δ*ortR* was made using a two-step
326 transformation method as described previously [51]. Briefly, approximately 1 kb of the
327 homologous sequence upstream and downstream of the *ortR* open reading frame (ORF)
328 was amplified from *S. mutans* UA159 genomic DNA using PCR with the upF/upR and
329 dnF/dnR primers and the selection cassette IFDC2 (positive for erythromycin and negative
330 for *p*-Cl-phe) was amplified by the *ldh*F/*erm*R primers, respectively. Then, the fragments
331 containing the overlapping regions were ligated using the overlap extension PCR with
332 upF/dnR primers, which were transformed into *S. mutans* UA159 and selected by using

333 BHI agar plate containing erythromycin (12 μg/mL). For the second transformation,
334 upstream and downstream fragments of *ortR* were amplified using the primer upF/updnR
335 and dnF/dnR and ligated using the primer upF/dnR. The ligated fragment was transformed
336 into the first-step constructed mutant strain and selected by using plates containing *p*-Cl-
337 phe (4 mg/mL, Sigma, United States). Finally, the markerless in-frame deletion mutant was
338 further confirmed by PCR and sequencing.
339

340 Quantitative reverse transcription polymerase chain reaction

341 Quantitative reverse transcription polymerase chain reaction (qRT-PCR) was used to
342 quantify the expression of the *ortR* gene in overexpression and deletion strains. Bacterial
343 cells were cultured to the mid-logarithmic phase (OD_{600nm}=0.5), harvested by
344 centrifugation (4, 000 g, 4℃, 10 min), and frozen in liquid nitrogen until use. To evaluate
345 the gene expression of overexpression and deletion strains of the *ortR* gene. Primer3 online
346 tool (http://simgene.com/Primer3) was used to design the specific primer of *ortR* gene. The
347 separation, purification and reverse transcription of bacterial total RNA were carried out
348 according to the instructions. Additionally, 16S ribosomal RNA (rRNA) gene was used as
349 an internal control and the data were analyzed according to the $2^{-\Delta\Delta CT}$ method.
350

351 Growth curve assay

352 Overnight cultures of *S. mutans* and its derivatives were subcultured at a dilution of 1:10
353 in BHI medium until the optical density (OD) at 600nm (OD_{600nm}) to 0.5. The cultured cells

354 were diluted by 1:100 and inoculated in the 96-well cell culture plates (Corning, NY,
355 United States) with each well covered by sterile mineral oil. The OD_{600nm} was measured
356 using a spectrophotometer (BioTek, Winooski, VT, United States) at 30-min intervals for
357 12h as described previously [35].
358

359 ## Biofilm formation assay

360 The crystal violet staining method was used to assess the biofilm biomass as described
361 previously [52]. Briefly, the subcultured cells were diluted by 1:100 with BHIS and
362 aerobically cultured in 24-well cell culture plates (Corning, NY, United States). After 24-
363 h incubation, the growth medium was gently removed, and the biofilm was rinsed three
364 times with sterile phosphate-buffered saline (PBS) and stained with 0.01% CV (wt/vol) for
365 15 min. Then, the wells were rinsed three times with PBS and eluted with 33% acetic acid
366 for 30min. The absorbance of the solution was measured at OD_{575nm} by spectrophotometer.
367

368 ## Glycolytic pH drop and acid killing assays

369 The ability of *S. mutans* to lower the pH through glycolysis was monitored as described
370 previously with some modifications [53]. Briefly, *S. mutans* and its derivatives were
371 harvested until OD_{600nm} to 0.5, rinsed with 1 mL PBS solution, and resuspended in the salt
372 solution containing 50 mM KCl and 1 mM $MgCl_2$ (pH=7.0). pH drop was initiated by
373 adding 1% (wt/vol) glucose and monitored at 5- or 10-min intervals for 60 min using the
374 Orion Dual Star, pH/ISE Benchtop (Thermo Scientific, Waltham, MA).

375 The acid killing assay was performed as described previously to test their acid
376 resistance ability [54]. Similar procedures with pH drop assay, *S. mutans* and its derivatives
377 were harvested until OD_{600nm} to 0.5. Cell pellets were rinsed once with 0.1-M glycine
378 (pH=7.0), centrifuged again, and resuspended in 0.1-M glycine (pH=2.8) for acid killing.
379 Aliquots were taken at 0, 15, 30, and 45 min and then serially diluted and cultured on the
380 BHI agar plates for enumeration of the colony-forming units (CFUs).
381

382 **Hydrogen peroxide killing and sensitivity assays**

383 The ability of bacterial strains to withstand hydrogen peroxide challenge was determined
384 using protocols described elsewhere [55]. The procedures for measuring hydrogen
385 peroxide tolerance were similar to measuring acid tolerance, except that hydrogen peroxide
386 tolerance was assessed using 0.2% (66.05mM) hydrogen peroxide for 0, 20, 40, and 60 min,
387 respectively.

388 The hydrogen peroxide sensitivity assay was performed as follows: overnight cultures
389 of *S. mutans* and its derivatives were washed and adjusted to the OD_{600nm} of 0.5. Four
390 milliliters of molten BHI-soft-agar (0.6% agar, 60°C) were thoroughly mixed with 200 μL
391 of *S. mutans* and its derivatives cell suspension and immediately poured onto the BHI agar
392 plates, which were kept at room temperature for 30 min. Subsequently, the filter discs
393 containing 0-, 20-, 40-, and 60-mM hydrogen peroxide were added to BHI-soft-agar plates
394 of the test strains followed by 24 h of incubation at 37°C. Inhibition zones were measured
395 at three different positions and averaged to a single datapoint and the ratio of inhibition

396 zone to disc diameter was calculated.

397

398 Bacterial composition analysis in three-species biofilms

399 Overnight cultures of *S. mutans* and its derivatives, *S. gordonii*, and *S. sanguinis* were
400 harvested until OD_{600nm} to 0.5, and simultaneously inoculated (inoculum ratio of *S.*
401 *mutans*/*S. gordonii/S. sanguinis*=1:1:1) in fresh BHIS or supplemented with 3 mg/mL
402 catalase under aerobic conditions for 24 h. Then, the 24-h three-species biofilms were fixed
403 with 4% paraformaldehyde (PFA) and labeled by species-specific fluorescent *in situ*
404 hybridization (FISH) probes, as previously described with some modifications [33].
405 Biofilm images were captured using an Olympus FV3000 confocal laser scanning
406 microscope (Olympus Corporation, Tokyo, Japan) at 60× magnification from at least five
407 randomly selected positions of each sample. The three-dimensional structure of the three-
408 species biofilms was reconstructed by IMARIS 7.0.0 (Bitplane, Zurich, Switzerland), and
409 the Image-Pro Plus 6.0 (Media Cybernetics) software was used to analyze the bacterial
410 composition.

411

412 RNA-sequencing

413 For RNA-sequencing, the subcultured UA159/pDL278 and UA159/pDL278-*ortR* strains
414 were harvested until OD_{600nm} to 0.5 under aerobic conditions, and snap frozen in liquid
415 nitrogen until needed as described previously [56]. Total RNA from three independent
416 samples was exacted and purified using TRIzol reagent according to the manufacturer's

417 instructions (Invitrogen, United States). RNA quality was determined by 2100 Bioanalyzer
418 (Agilent, United States) and the RNA concentration was quantified using an ND-2000
419 instrument (NanoDrop Technologies, United States). cDNA library was constructed from
420 enriched mRNA samples using the TruSeq RNA sample prep kit (Illumina, San Diego,
421 CA, United States). rRNA depletion from total RNA was performed using the Ribo-Zero
422 magnetic kit (Epicentre Biotechnologies, United States) and the mRNA was chemically
423 fragmented to short pieces (200 nt) using a 1 × fragmentation solution (Ambion, United
424 States) for 2.5 min at 94°C. Double-stranded cDNA was produced using the SuperScript
425 double-stranded cDNA synthesis kit (Invitrogen) with random hexamer primers (Illumina).
426 Then, the synthesized cDNA was subjected to end repair, phosphorylation, and "A" base
427 addition according to Illumina's library construction protocol. Libraries were selected for
428 cDNA target fragments of 200 bp on 2% low-range Ultra agarose followed by PCR
429 amplification using Phusion DNA polymerase (NEB, United States) for 15 PCR cycles.
430 After quantification by TBS380, the paired-end RNA-seq sequencing library was
431 sequenced with the Illumina HiSeq X Ten instrument (2 × 150-bp read length). Genes with
432 a 2-fold difference and a P-value < 0.05 were selected as differentially expressed genes
433 (DEGs). Functional annotation and enrichment analysis of DEGs were performed in Gene
434 Ontology (GO) and Kyoto Encyclopedia of Genes and genomes (KEGG) databases.
435

436 **Cloning, expression, and purification of recombinant OrtR**
437 **protein**

438 *ortR* was amplified from *S. mutans* genomic DNA and purified, digested by *EcoR*I and
439 *Xba*I, and cloned into the expression vector pET28a (Novagen) with an N-terminal fusion
440 of 6 × His-tag. The reconstructed plasmid was cloned to the *Escherichia coli* strain BL21
441 (DE3) cells. Then, overnight cultures of the transformant were diluted at 1:20 with fresh
442 LB medium containing 50 μg/mL kanamycin until OD_{600nm} to 0.6. After further growth
443 with 1 mM isopropyl-β-D-thiogalactopyranoside (IPTG) at 37°C for 6 h, which induced
444 protein expression, the cell pellets were harvested and lysed by sonification. Then, the
445 recombinant ActG was purified using a His-tagged protein purification kit (Beyotime,
446 Shanghai, China) following the manufacturer's protocol, and concentrated by 10 kDa
447 MWKO ultra-filtration (Millipore Amincon, Merck, Germany) from the cell debris as
448 described previously [52]. Purified OrtR concentration was determined by measuring its
449 spectrophotometric absorbance at 280 nm, further confirmed by SDS-PAGE, and stored at
450 -80ºC for future use.

451

452 **Electrophoretic mobility shift and DNase I footprinting assays**

453 Electrophoretic mobility shift assay (EMSA) was performed to confirm the DNA binding
454 activity and specificity of OrtR using protocols described previously with some
455 modifications [35]. Briefly, DNA fragments containing *smu_137 promoter* (116 bp),
456 *smu_136c* ORF (116 bp), *smu_764* promoter (131 bp), and *smu_765* ORF (131 bp) were

457 amplified by PCR using the primer listed in S2 Table. The 49 bp oligonucleotides *smu_137*
458 promoter containing the putative binding motif of OrtR and *smu_137* promoter mut
459 containing mutant oligonucleotide site (A and T bases were changed to C and G,
460 respectively) within the putative binding motif of OrtR were labeled with 5-
461 carboxyfluorescein (FAM) and annealed with the complementary strand by heating to
462 95°C for 5 min and cooling to room temperature. Then, DNA fragments were incubated
463 with recombinant OrtR protein in the binding buffer of 50 mM Tris/HCl, 10 mM NaCl, 0.5
464 M Mg/acetate, 0.1 mM EDTA, and 5% (vol/vol) glycerol for 30 min on ice. DNA-protein
465 complexes were separated by non-denaturing polyacrylamide gel electrophoresis at 110 V
466 for 60 min. The gels were dyed with Ethidium Bromide (Thermo Scientific, Waltham, MA,
467 US) for 20 min, and images were captured using a ChemiDoc touch imaging system (Bio-
468 Rad, United States).

469 DNase I footprinting assay was used to determining the specific binding motif of OrtR
470 under similar conditions to those described for EMSA analysis. Briefly, the *smu_137*
471 promoter region was amplified using specific primers labeled with FAM. After purification,
472 DNA fragment (112.5 nM) was mixed with recombinant OrtR (0, 2.5, 7.5, 12.5 μM), which
473 was treated with DNase I (1 unit, Solarbio) at 37°C for 5 min. Then, the reaction was
474 stopped using phenol chloroform, and DNA fragments were precipitated with ethanol, and
475 eluted in 15 μL distilled water. The obtained fragment was analyzed using a 3730XL DNA
476 analyzer (Applied Biosystems, Tsingke, China). Electropherograms were analyzed and
477 aligned using GENEMAPPER software (Thermo Fisher Scientific, United States). The

478 protected sequence was used to search for other matched binding motifs of OrtR in the
479 downregulated gene clusters using the MEME Suite 5.1.1.
480

481 ## Statistical analysis

482 Statistical analysis was performed with SPSS 20.0 (SPSS Software Inc, Chicago, IL, USA).
483 Data are presented as means ± SDs from three biological replicates performed in triplicate.
484 The student's test was used to compare data between two groups. Analysis of variance and
485 Tukey's test were performed to compare data between multiple groups. $P < 0.05$ was
486 considered statistically significant.
487

488 # Acknowledgments

489 We are thankful fo Jumei Zeng for their technical assistance in electrophoretic mobility
490 shift and DNase I footprinting assays.
491

492 # References

493 1. Kassebaum NJ, Bernabé E, Dahiya M, Bhandari B, Murray CJL, Marcenes W. Global
494 burden of untreated caries: a systematic review and metaregression. J Dent Res.
495 2015;94: 650–658. doi:10.1177/0022034515573272
496 2. Pitts NB, Zero DT, Marsh PD, Ekstrand K, Weintraub JA, Ramos-Gomez F, et al.
497 Dental caries. Nat Rev Dis Primers. 2017;3: 17030. doi:10.1038/nrdp.2017.30
498 3. Marsh PD. Dental plaque as a biofilm and a microbial community-implications for
499 health and disease. BMC Oral Health. 2006;6 Suppl 1: S14. doi:10.1186/1472-6831-
500 6-S1-S14
501 4. Bowen WH, Koo H. Biology of *Streptococcus mutans*-derived glucosyltransferases:
502 role in extracellular matrix formation of cariogenic biofilms. Caries Res. 2011;45: 69–
503 86. doi:10.1159/000324598
504 5. Loesche WJ. Role of *Streptococcus mutans* in human dental decay. Microbiol Rev.
505 1986;50: 353–380.
506 6. Pant S, Patel NJ, Deshmukh A, Golwala H, Patel N, Badheka A, et al. Trends in
507 infective endocarditis incidence, microbiology, and valve replacement in the United
508 States from 2000 to 2011. J Am Coll Cardiol. 2015;65: 2070–2076.
509 doi:10.1016/j.jacc.2015.03.518
510 7. Tuganbaev T, Yoshida K, Honda K. The effects of oral microbiota on health. Science.
511 2022;376: 934–936. doi:10.1126/science.abn1890
512 8. Wang C, Van Der Mei HC, Busscher HJ, Ren Y. *Streptococcus mutans* adhesion force

513 sensing in multi-species oral biofilms. npj Biofilms Microbiomes. 2020;6: 25.
514 doi:10.1038/s41522-020-0135-0
515 9. Elias S, Banin E. Multi-species biofilms: living with friendly neighbors. FEMS
516 Microbiol Rev. 2012;36: 990–1004. doi:10.1111/j.1574-6976.2012.00325.x
517 10. Miller DP, Fitzsimonds ZR, Lamont RJ. Metabolic signaling and spatial interactions
518 in the oral polymicrobial community. J Dent Res. 2019;98: 1308–1314.
519 doi:10.1177/0022034519866440
520 11. Lamont RJ, Koo H, Hajishengallis G. The oral microbiota: dynamic communities and
521 host interactions. Nat Rev Microbiol. 2018;16: 745–759. doi:10.1038/s41579-018-
522 0089-x
523 12. Peterson SN, Meissner T, Su AI, Snesrud E, Ong AC, Schork NJ, et al. Functional
524 expression of dental plaque microbiota. Front Cell Infect Microbiol. 2014;4: 108.
525 doi:10.3389/fcimb.2014.00108
526 13. Boles BR, Singh PK. Endogenous oxidative stress produces diversity and adaptability
527 in biofilm communities. Proc Natl Acad Sci U S A. 2008;105: 12503–12508.
528 doi:10.1073/pnas.0801499105
529 14. Marquis R. Oxygen metabolism, oxidative stress and acid-base physiology of dental
530 plaque biofilms. Journal of Industrial Microbiology. 1995;15: 198–207.
531 doi:10.1007/BF01569826
532 15. Sies H, Belousov VV, Chandel NS, Davies MJ, Jones DP, Mann GE, et al. Defining
533 roles of specific reactive oxygen species (ROS) in cell biology and physiology. Nat

534 Rev Mol Cell Biol. 2022;23: 499–515. doi:10.1038/s41580-022-00456-z

535 16. Kajfasz JK, Zuber P, Ganguly T, Abranches J, Lemos JA. Increased oxidative stress
536 tolerance of a spontaneously occurring *perr* gene mutation in *Streptococcus mutans*
537 UA159. J Bacteriol. 2021;203. doi:10.1128/JB.00535-20

538 17. Borisov VB, Siletsky SA, Nastasi MR, Forte E. ROS defense systems and terminal
539 oxidases in bacteria. Antioxidants (Basel). 2021;10: 839.
540 doi:10.3390/antiox10060839

541 18. Juan CA, Pérez de la Lastra JM, Plou FJ, Pérez-Lebeña E. The Chemistry of reactive
542 oxygen species (ROS) revisited: outlining their role in biological macromolecules
543 (dna, lipids and proteins) and induced pathologies. Int J Mol Sci. 2021;22: 4642.
544 doi:10.3390/ijms22094642

545 19. Imlay JA. The molecular mechanisms and physiological consequences of oxidative
546 stress: lessons from a model bacterium. Nat Rev Microbiol. 2013;11: 443–454.
547 doi:10.1038/nrmicro3032

548 20. Dmitriev A, Mohapatra SS, Chong P, Neely M, Biswas S, Biswas I. CovR-controlled
549 global regulation of gene expression in *Streptococcus mutans*. PLoS One. 2011;6:
550 e20127. doi:10.1371/journal.pone.0020127

551 21. Biswas I, Mohapatra SS. CovR alleviates transcriptional silencing by a nucleoid-
552 associated histone-like protein in *Streptococcus mutans*. J Bacteriol. 2012;194: 2050–
553 2061. doi:10.1128/JB.06812-11

554 22. Ahn S-J, Rice KC. Understanding the *Streptococcus mutans* Cid/Lrg system through

555 CidB function. Appl Environ Microbiol. 2016;82: 6189–6203.
556 doi:10.1128/AEM.01499-16
557 23. Wang Y, Cao W, Merritt J, Xie Z, Liu H. Characterization of FtsH essentiality in
558 *Streptococcus mutans* via genetic suppression. Front Genet. 2021;12: 659220.
559 doi:10.3389/fgene.2021.659220
560 24. Ajdić D, McShan WM, McLaughlin RE, Savić G, Chang J, Carson MB, et al. Genome
561 sequence of *Streptococcus mutans* UA159, a cariogenic dental pathogen. Proc Natl
562 Acad Sci USA. 2002;99: 14434–14439. doi:10.1073/pnas.172501299
563 25. Humphrey S, Fillol-Salom A, Quiles-Puchalt N, Ibarra-Chávez R, Haag AF, Chen J,
564 et al. Bacterial chromosomal mobility via lateral transduction exceeds that of classical
565 mobile genetic elements. Nat Commun. 2021;12: 6509. doi:10.1038/s41467-021-
566 26004-5
567 26. Dobrindt U, Hochhut B, Hentschel U, Hacker J. Genomic islands in pathogenic and
568 environmental microorganisms. Nat Rev Microbiol. 2004;2: 414–424.
569 doi:10.1038/nrmicro884
570 27. Waterhouse JC, Russell RRB. Dispensable genes and foreign DNA in *Streptococcus*
571 *mutans*. Microbiology. 2006;152: 1777–1788. doi:10.1099/mic.0.28647-0
572 28. Wu C, Cichewicz R, Li Y, Liu J, Roe B, Ferretti J, et al. Genomic island TnSmu2 of
573 *Streptococcus mutans* harbors a nonribosomal peptide synthetase-polyketide synthase
574 gene cluster responsible for the biosynthesis of pigments involved in oxygen and H_2O_2
575 tolerance. Appl Environ Microbiol. 2010;76: 5815–5826. doi:10.1128/AEM.03079-

576 09

577 29. Kreth J, Merritt J, Shi W, Qi F. Competition and coexistence between *Streptococcus*
578 *mutans* and *Streptococcus sanguinis* in the dental biofilm. J Bacteriol. 2005;187:
579 7193–7203. doi:10.1128/JB.187.21.7193-7203.2005

580 30. Zheng W, Tan MF, Old LA, Paterson IC, Jakubovics NS, Choo SW. Distinct
581 Biological potential of *Streptococcus gordonii* and *Streptococcus sanguinis* revealed
582 by comparative genome analysis. Sci Rep. 2017;7: 2949. doi:10.1038/s41598-017-
583 02399-4

584 31. Tong H, Chen W, Merritt J, Qi F, Shi W, Dong X. *Streptococcus oligofermentans*
585 inhibits *Streptococcus mutans* through conversion of lactic acid into inhibitory H_2O_2:
586 a possible counteroffensive strategy for interspecies competition. Mol Microbiol.
587 2007;63: 872–880. doi:10.1111/j.1365-2958.2006.05546.x

588 32. Liu L, Tong H, Dong X. Function of the pyruvate oxidase-lactate oxidase cascade in
589 interspecies competition between *Streptococcus oligofermentans* and *Streptococcus*
590 *mutans*. Appl Environ Microbiol. 2012;78: 2120–2127. doi:10.1128/AEM.07539-11

591 33. Cheng X, Zheng X, Zhou X, Zeng J, Ren Z, Xu X, et al. Regulation of oxidative
592 response and extracellular polysaccharide synthesis by a diadenylate cyclase in
593 *Streptococcus mutans*. Environ Microbiol. 2016;18: 904–922. doi:10.1111/1462-
594 2920.13123

595 34. Lu M, Xiang Z, Gong T, Zhou X, Zhang Z, Tang B, et al. Intrinsic fluoride tolerance
596 regulated by a transcription factor. J Dent Res. 2020;99: 1270–1278.

597 doi:10.1177/0022034520927385

598 35. Chen J, Zhang A, Xiang Z, Lu M, Huang P, Gong T, et al. EpsR negatively regulates
599 *Streptococcus mutans* exopolysaccharide synthesis. J Dent Res. 2021;100: 968–976.
600 doi:10.1177/00220345211000668

601 36. Tinder EL, Faustoferri RC, Buckley AA, Quivey RG, Baker JL. Analysis of the
602 *Streptococcus mutans* proteome during acid and oxidative stress reveals modules of
603 protein coexpression and an expanded role for the TreR transcriptional regulator.
604 mSystems. 2022;7: e0127221. doi:10.1128/msystems.01272-21

605 37. Paster BJ, Boches SK, Galvin JL, Ericson RE, Lau CN, Levanos VA, et al. Bacterial
606 diversity in human subgingival plaque. J Bacteriol. 2001;183: 3770–3783.
607 doi:10.1128/JB.183.12.3770-3783.2001

608 38. Aas JA, Paster BJ, Stokes LN, Olsen I, Dewhirst FE. Defining the normal bacterial
609 flora of the oral cavity. J Clin Microbiol. 2005;43: 5721–5732.
610 doi:10.1128/JCM.43.11.5721-5732.2005

611 39. Kaspar JR, Lee K, Richard B, Walker AR, Burne RA. Direct interactions with
612 commensal streptococci modify intercellular communication behaviors of
613 *Streptococcus mutans*. ISME J. 2021;15: 473–488. doi:10.1038/s41396-020-00789-7

614 40. Kolenbrander PE, Palmer RJ, Periasamy S, Jakubovics NS. Oral multispecies biofilm
615 development and the key role of cell–cell distance. Nat Rev Microbiol. 2010;8: 471–
616 480. doi:10.1038/nrmicro2381

617 41. Kreth J, Zhang Y, Herzberg MC. Streptococcal antagonism in oral biofilms:

618 *Streptococcus sanguinis* and *Streptococcus gordonii* interference with *Streptococcus*
619 *mutans*. Journal of Bacteriology. 2008;190: 4632. doi:10.1128/JB.00276-08
620 42. Zhu L, Kreth J. The role of hydrogen peroxide in environmental adaptation of oral
621 microbial communities. Oxidative Medicine and Cellular Longevity. 2012;2012: 1–
622 10. doi:10.1155/2012/717843
623 43. De Furio M, Ahn SJ, Burne RA, Hagen SJ. Oxidative stressors modify the response
624 of *Streptococcus mutans* to its competence signal peptides. Appl Environ Microbiol.
625 2017;83: e01345-17. doi:10.1128/AEM.01345-17
626 44. Lemos J, Palmer S, Zeng L, Wen Z, Kajfasz J, Freires I, et al. The biology of
627 *Streptococcus mutans*. Microbiol Spectr. 2019;7: 10.1128/microbiolspec.GPP3-
628 0051–2018. doi:10.1128/microbiolspec.GPP3-0051-2018
629 45. Ramos JL, Martínez-Bueno M, Molina-Henares AJ, Terán W, Watanabe K, Zhang X,
630 et al. The TetR family of transcriptional repressors. Microbiol Mol Biol Rev. 2005;69:
631 326–356. doi:10.1128/MMBR.69.2.326-356.2005
632 46. Cuthbertson L, Nodwell JR. The TetR family of regulators. Microbiol Mol Biol Rev.
633 2013;77: 440–475. doi:10.1128/MMBR.00018-13
634 47. Chattoraj P, Mohapatra SS, Rao JLUM, Biswas I. Regulation of transcription by
635 SMU.1349, a TetR family regulator, in *Streptococcus mutans*. J Bacteriol. 2011;193:
636 6605–6613. doi:10.1128/JB.06122-11
637 48. Lyu M, Cheng Y, Han X, Wen Y, Song Y, Li J, et al. AccR, a TetR family
638 transcriptional repressor, coordinates short-chain acyl coenzyme a homeostasis in

639 *Streptomyces avermitilis*. Appl Environ Microbiol. 2020;86: e00508-20.
640 doi:10.1128/AEM.00508-20
641 49. Xu S, Jiang Y, Zhang F, Wang X, Zhang K, Zhao L, et al. The TetR family repressor
642 HpaR negatively regulates the catabolism of 5-hydroxypicolinic acid in *Alcaligenes*
643 *faecalis* JQ135 by binding to two unique dna sequences in the promoter of Hpa operon.
644 Appl Environ Microbiol. 2022;88: e0239021. doi:10.1128/aem.02390-21
645 50. Ma Q, Pan Y, Chen Y, Yu S, Huang J, Liu Y, et al. Acetylation of glucosyltransferases
646 regulates *Streptococcus mutans* biofilm formation and virulence. PLoS Pathog.
647 2021;17: e1010134. doi:10.1371/journal.ppat.1010134
648 51. Xie Z, Okinaga T, Qi F, Zhang Z, Merritt J. Cloning-independent and
649 counterselectable markerless mutagenesis system in *Streptococcus mutans*. Appl
650 Environ Microbiol. 2011;77: 8025–8033. doi:10/djs3s8
651 52. Pan Y, Chen Y, Chen J, Ma Q, Gong T, Yu S, et al. The Adc regulon mediates zinc
652 homeostasis in *Streptococcus mutans*. Mol Oral Microbiol. 2021;36: 278–290.
653 doi:10.1111/omi.12350
654 53. Belli WA, Marquis RE. Adaptation of *Streptococcus mutans* and *Enterococcus hirae*
655 to acid stress in continuous culture. Appl Environ Microbiol. 1991;57: 1134–1138.
656 doi:10.1128/aem.57.4.1134-1138.1991
657 54. Ma Q, Pan Y, Chen Y, Yu S, Huang J, Liu Y, et al. Acetylation of lactate
658 dehydrogenase negatively regulates the acidogenicity of *Streptococcus mutans*. mBio.
659 2022; e0201322. doi:10.1128/mbio.02013-22

660 55. Redanz S, Treerat P, Mu R, Redanz U, Zou Z, Koley D, et al. Pyruvate secretion by
661 oral streptococci modulates hydrogen peroxide dependent antagonism. ISME J.
662 2020;14: 1074–1088. doi:10.1038/s41396-020-0592-8
663 56. Gong T, He X, Chen J, Tang B, Zheng T, Jing M, et al. Transcriptional profiling
664 reveals the importance of RcrR in the regulation of multiple sugar transportation and
665 biofilm formation in *Streptococcus mutans*. mSystems. 2021;6: e0078821.
666 doi:10.1128/mSystems.00788-21
667

668 # Supporting information

669 **S1 Fig. Gene expression level of *ortR* in indicated strains.** Gene expression level of *ortR*
670 was determined by qRT-PCR and caculated using the 2-ΔΔCt method with values
671 nomalized to the reference gene 16s rRNA. The results are presented as mean ± SD (***
672 $P < 0.001$ or ** $P < 0.01$).

673

674 **S2 Fig. Effect of *ortR* on the acidogenesis and aciduricity of *S. mutans*.** (A) The
675 glycolytic pH drop was performed by monitoring the pH value of the supernatant of UA159,
676 UA159/pDL278, UA159/pDL278-*ortR*, and UA159 Δ*ortR* cultures grown in the presence
677 of 1% glucose over 60 min. (B) Exponential cultures of UA159, UA159/pDL278,
678 UA159/pDL278-*ortR*, and UA159 Δ*ortR* were exposed to acid stress at pH 2.8 for 0, 15,
679 30, and 45 min, respectively, which were serially diluted and cultured on the BHI agar
680 plates.

681

682 **S1 Table. Bacterial strains and plasmids used in this study.**

683

684 **S2 Table. Primers used in this study.**

685

686 **S3 Table. List of genes downregulated greater than 2.0-fold.**

687

688 **S4 Table. List of genes upregulated greater than 2.0-fold.**

689

690 **S5 Table. Gene-annotation enrichment analysis of differentially regulated genes in**

691 **KEGG pathway using DAVID tools (*P* < 0.05).**

692

693 **S6 Table. Gene-annotation enrichment analysis of differentially regulated genes in**

694 **GO terms using DAVID tools (*P* < 0.05).**

695

696 Figure legends

697 **Fig 1. Effect of *ortR* on the growth, biofilm formation, and oxidative tolerance of *S.***

698 ***mutans*.** (A) Growth characteristics of UA159, UA159/pDL278, UA159/pDL278-*ortR*,

699 and UA159 Δ*ortR*. Bacteria were grown aerobically at 37°C, and OD_{600nm} was monitored

700 at 30-min intervals for 12 h. (B) The biofilm biomass was determined using crystal violet

701 staining assay when bacteria were cultured in BHIS under aerobic conditions for 6, 12, and

702 24 h, respectively. The exponential cultures of UA159, UA159/pDL278, UA159/pDL278-

703 *ortR*, and UA159 Δ*ortR* were exposed to oxidative stress with 0.2% (66.05mM) hydrogen

704 peroxide for 0, 20, 40, and 60 min, respectively, which were serially diluted and cultured

705 on the BHI agar plates. The representative pictures of the hydrogen peroxide challenge are

706 shown (C), and colony-forming units (CFUs) were counted, and percent survivals of

707 different strains were calculated relative to the control sample UA159 (D). The plates were

708 overlaid with soft agar containing UA159, UA159/pDL278, UA159/pDL278-*ortR*, and

709 UA159 Δ*ortR* and challenged with filter discs soaked with 0-, 20-, 40-, and 60-mM

710 hydrogen peroxide. The representative plates are shown to demonstrate the differences in
711 inhibition zones (E), which are measured at three different positions and averaged to serve
712 as a single datapoint, and the ratio of inhibition zone to disc diameter was calculated (F).
713 Each experiment was repeated at least thrice. Results are presented as mean ± SD (* $P <$
714 0.05 or *** $P < 0.001$).

715

716 **Fig 2. Effect of *ortR* on interspecies competition within the three-species biofilms.** *S.*
717 *mutans* and its derivatives, *S. gordonii*, and *S. sanguinis* were simultaneously cultured in
718 fresh BHIS (A, B) or supplemented with 3 mg/mL catalase (C, D) under aerobic conditions
719 for 24 h and labeled by species-specific fluorescent *in situ* hybridization (FISH) probes.
720 The three-dimensional visualization of three-species biofilms with *S. mutans* (green), *S.*
721 *gordonii* (blue), and *S. sanguinis* (red) was captured using the confocal laser scanning
722 microscopy (CLSM) at 60× magnification and reconstructed using the IMARIS 7.0.0 (A,
723 C). The ratio of *S. mutans*/*S. gordonii*/*S. sanguinis* was quantified by the coverage area of
724 each species with Image Pro Plus 6.0 (B, D). The representative images are shown from at
725 least five randomly selected positions of each sample. Results are presented as mean ± SD
726 (* $P < 0.05$ or **** $P < 0.0001$).

727

728 **Fig 3. Transcriptomics analysis of UA159/pDL278 and UA159/pDL278-*ortR* strains.**
729 (A) Functional classification of differentially expressed genes (DEGs) was performed
730 based on the clusters of orthologous groups (COG) type. (B) The volcano plot illustrates
731 DEGs between UA159/pDL278 and UA159/pDL278-*ortR*. Functional annotation and
732 enrichment analysis of DEGs were performed in the Kyoto Encyclopedia of Genes and
733 Genomes (KEGG, C) and Gene Ontology (GO, D) databases. Downregulated genes are
734 shown in green. (E) Genetic organization of gene clusters that were significantly
735 downregulated in UA159/pDL278-*ortR*.

736

737 **Fig 4. Identification of the promoter bound by OrtR.** DNA substrates were incubated
738 with different concentrations of OrtR protein, which was analyzed using EMSA. The
739 results show that OrtR can directly bind to the promoter of *smu_137-smu_141* (A, lanes
740 1–4) and *smu_764-smu_765* (B, lanes 1–4) and cannot bind to *smu_136c* ORF (A, lanes
741 5–8) and *smu_765* ORF (B, lanes 5–8).

742

743 **Fig 5. Identification of the conserved DNA motif bound by OrtR.** (A) The *smu_137*
744 promoter labeled with FAM was incubated with increasing concentrations of OrtR protein.
745 DNase I footprinting assay was performed to identify the specific binding motif, which
746 was protected by OrtR protein from DNase I digestion and marked in red. (B) Two DNA
747 fragments containing the binding motif and its mutant motif were incubated with increasing

748 concentrations of OrtR protein, which was analyzed using EMSA. The results show that
749 OrtR can directly bind to *smu_137* promoter (lanes 1–4) and cannot bind to *smu_137*
750 promoter mut (lanes 5–8). (C) The putative OrtR binding motifs in the promoters of
751 significantly downregulated gene clusters were searched, and the sequence logo was
752 generated using MEME Suite 5.1.1 and WebLogo tool, respectively.

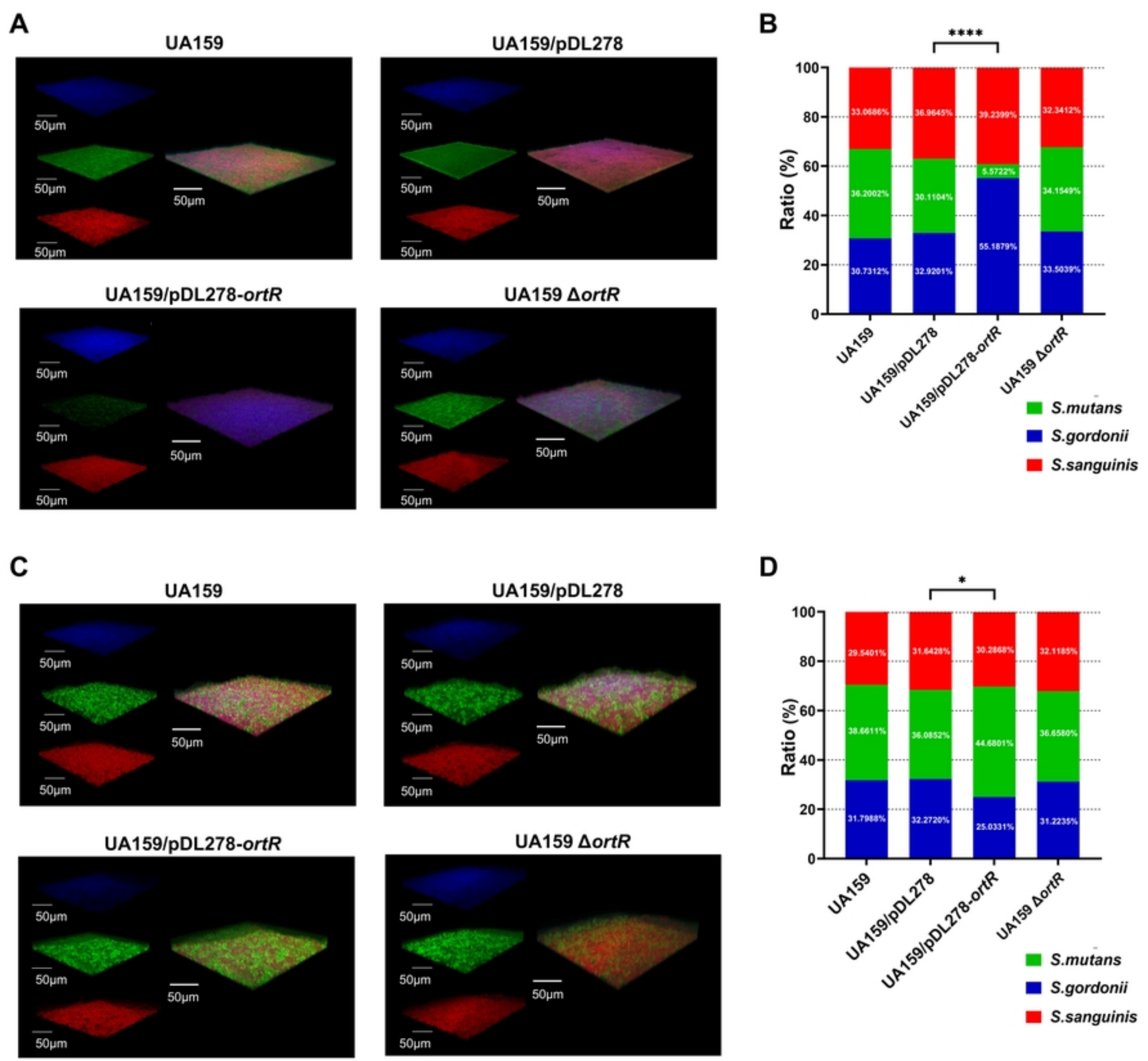
A
UA159
UA159/pDL278
UA159/pDL278-ortR
UA159 ΔortR
50μm
B
****
Ratio (%)
100
80
60
40
20
0
33.0686%
36.9645%
39.2399%
32.3412%
36.2002%
30.1104%
5.5722%
34.1549%
30.7312%
32.9201%
55.1879%
33.5039%
UA159
UA159/pDL278
UA159/pDL278-ortR
UA159 ΔortR
S.mutans
S.gordonii
S.sanguinis
C
D
*
29.5401%
31.6428%
30.2868%
32.1185%
38.6611%
36.0852%
44.6801%
36.6580%
31.7988%
32.2720%
25.0331%
31.2235%

Fig 2

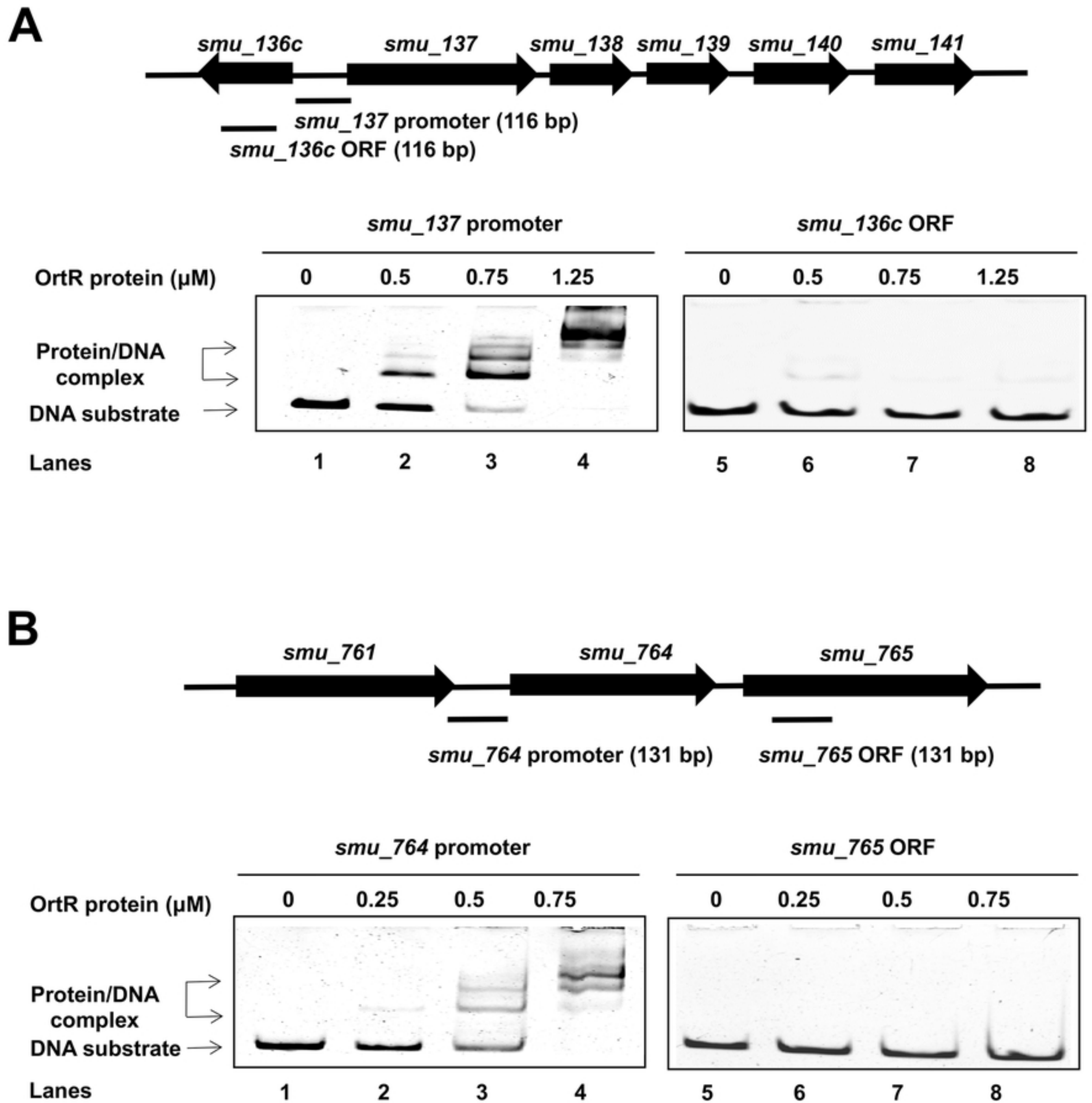
A
smu_136c
smu_137
smu_138
smu_139
smu_140
smu_141
smu_137 promoter (116 bp)
smu_136c ORF (116 bp)
smu_137 promoter
smu_136c ORF
OrtR protein (μM)
0
0.5
0.75
1.25
0
0.5
0.75
1.25
Protein/DNA complex
DNA substrate
Lanes
1
2
3
4
5
6
7
8
B
smu_761
smu_764
smu_765
smu_764 promoter (131 bp)
smu_765 ORF (131 bp)
smu_764 promoter
smu_765 ORF
OrtR protein (μM)
0
0.25
0.5
0.75
0
0.25
0.5
0.75
Protein/DNA complex
DNA substrate
Lanes
1
2
3
4
5
6
7
8

Fig 4

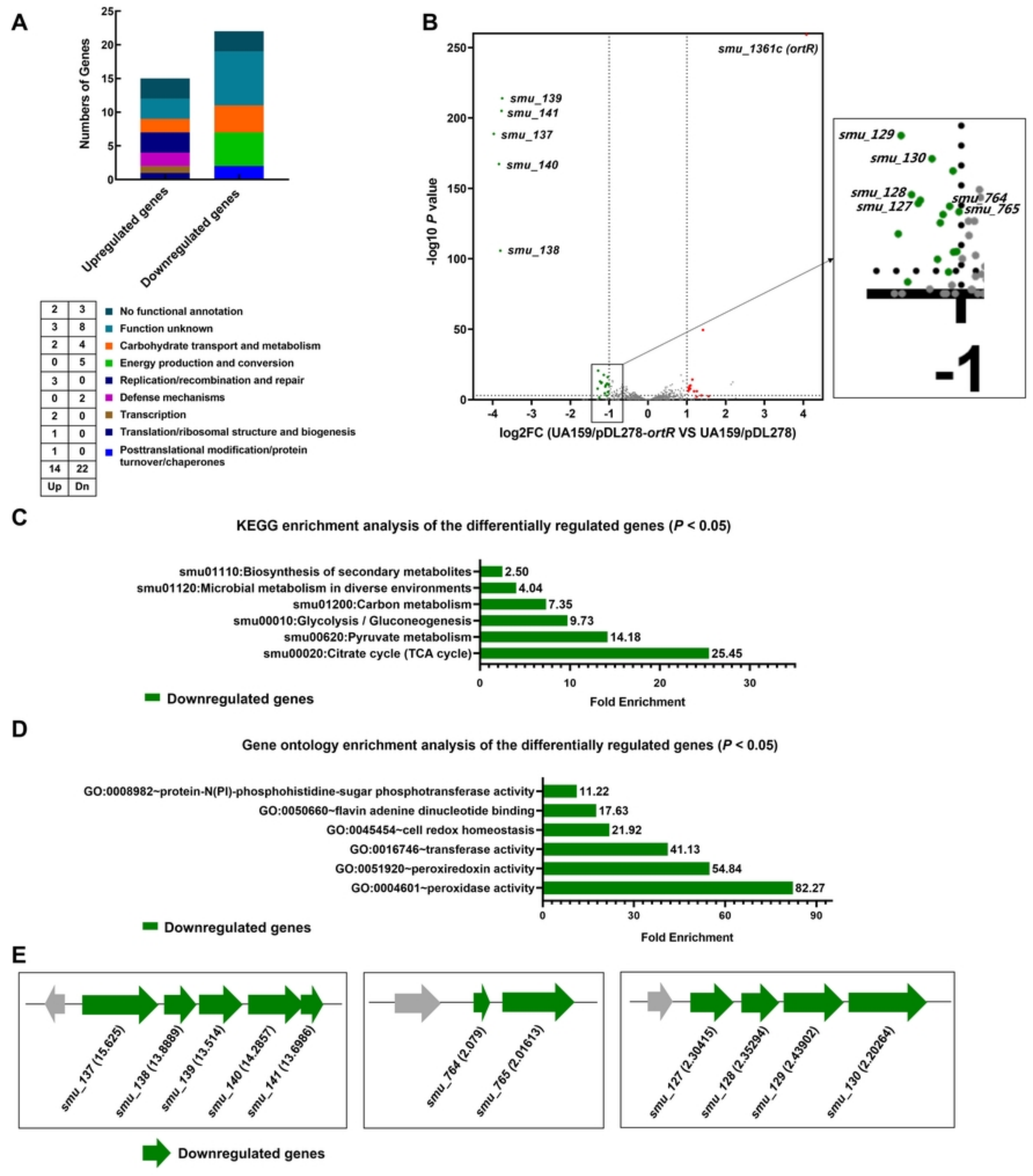
A
Numbers of Genes
Upregulated genes
Downregulated genes
No functional annotation
Function unknown
Carbohydrate transport and metabolism
Energy production and conversion
Replication/recombination and repair
Defense mechanisms
Transcription
Translation/ribosomal structure and biogenesis
Posttranslational modification/protein turnover/chaperones
Up
Dn
B
smu_1361c (ortR)
smu_139
smu_141
smu_137
smu_140
smu_138
smu_129
smu_130
smu_128
smu_127
smu_764
smu_765
-log10 P value
log2FC (UA159/pDL278-ortR VS UA159/pDL278)
C
KEGG enrichment analysis of the differentially regulated genes (P < 0.05)
smu01110:Biosynthesis of secondary metabolites
smu01120:Microbial metabolism in diverse environments
smu01200:Carbon metabolism
smu00010:Glycolysis / Gluconeogenesis
smu00620:Pyruvate metabolism
smu00020:Citrate cycle (TCA cycle)
2.50
4.04
7.35
9.73
14.18
25.45
Fold Enrichment
Downregulated genes
D
Gene ontology enrichment analysis of the differentially regulated genes (P < 0.05)
GO:0008982~protein-N(PI)-phosphohistidine-sugar phosphotransferase activity
GO:0050660~flavin adenine dinucleotide binding
GO:0045454~cell redox homeostasis
GO:0016746~transferase activity
GO:0051920~peroxiredoxin activity
GO:0004601~peroxidase activity
11.22
17.63
21.92
41.13
54.84
82.27
Fold Enrichment
Downregulated genes
E
smu_137 (15.625)
smu_138 (13.8889)
smu_139 (13.514)
smu_140 (14.2857)
smu_141 (13.6986)
smu_764 (2.079)
smu_765 (2.01613)
smu_127 (2.30415)
smu_128 (2.35294)
smu_129 (2.43902)
smu_130 (2.20264)
Downregulated genes

Fig 3

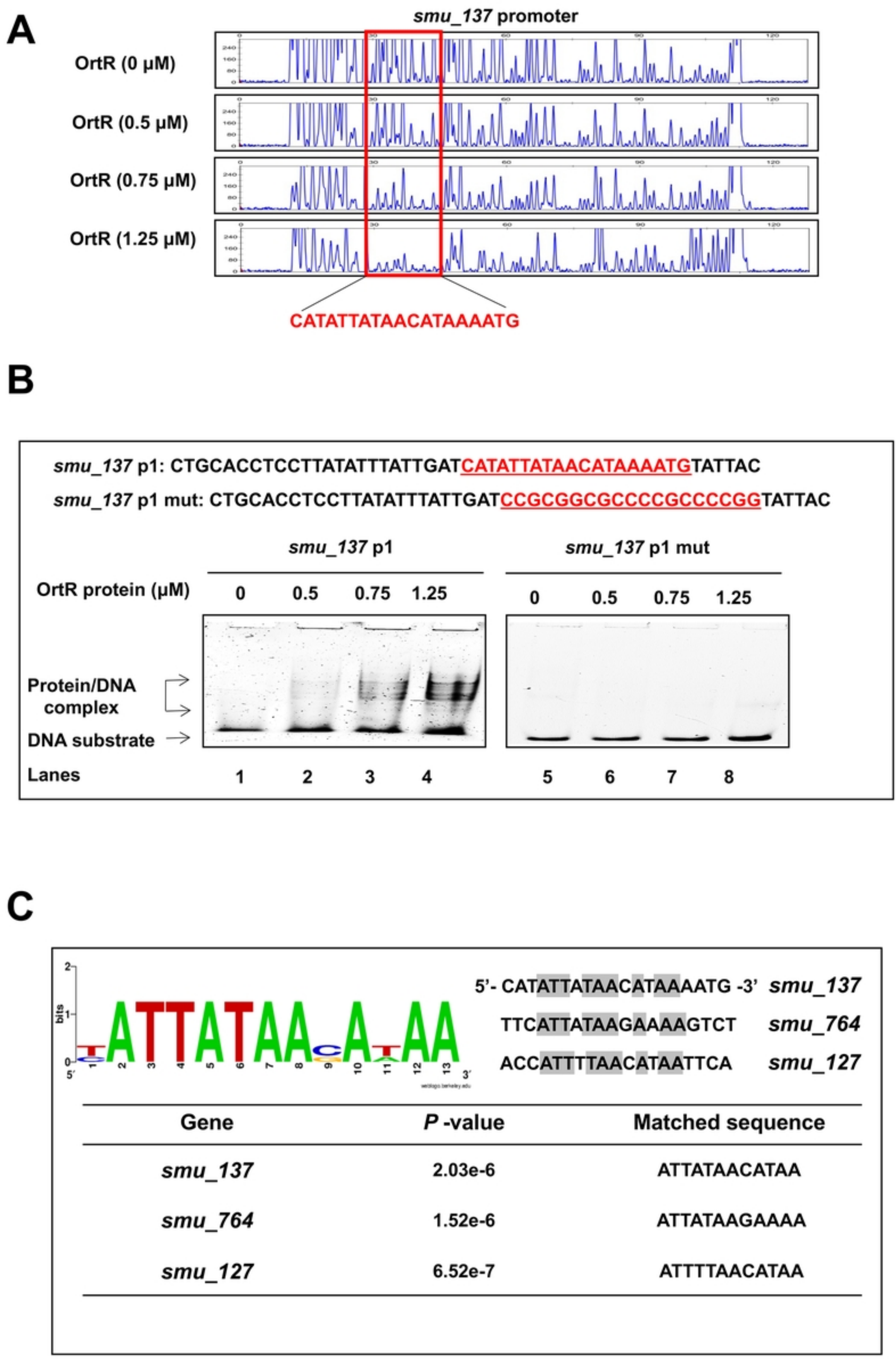
A
smu_137 promoter
OrtR (0 μM)
OrtR (0.5 μM)
OrtR (0.75 μM)
OrtR (1.25 μM)
CATATTATAACATAAAATG
B
smu_137 p1: CTGCACCTCCTTATATTTATTGATCATATTATAACATAAAATGTATTAC
smu_137 p1 mut: CTGCACCTCCTTATATTTATTGATCCGCGGCGCCCCGCCCCGGTATTAC
smu_137 p1
smu_137 p1 mut
OrtR protein (μM)
0 0.5 0.75 1.25
0 0.5 0.75 1.25
Protein/DNA complex
DNA substrate
Lanes
1 2 3 4 5 6 7 8
C
bits
5' 3'
5'- CATATTATAACATAAAATG -3' smu_137
TTCATTATAAGAAAAGTCT smu_764
ACCATTTTAACATAATTCA smu_127
Gene | P -value | Matched sequence
smu_137 | 2.03e-6 | ATTATAACATAA
smu_764 | 1.52e-6 | ATTATAAGAAAA
smu_127 | 6.52e-7 | ATTTTAACATAA

Fig 5

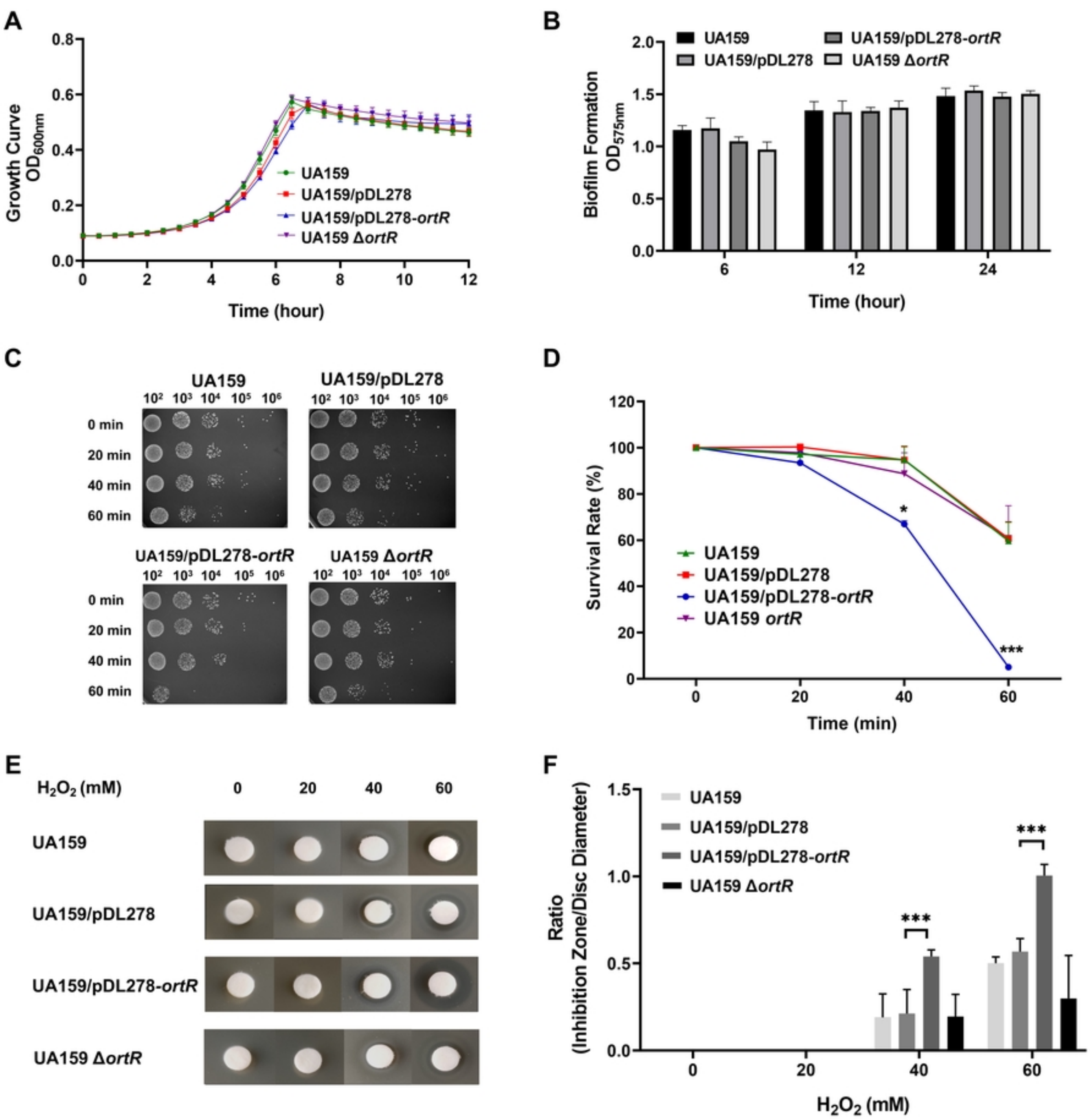
A
Growth Curve OD_{600nm}
Time (hour)
UA159
UA159/pDL278
UA159/pDL278-ortR
UA159 ΔortR
B
Biofilm Formation OD_{575nm}
Time (hour)
UA159
UA159/pDL278
UA159/pDL278-ortR
UA159 ΔortR
C
UA159
UA159/pDL278
UA159/pDL278-ortR
UA159 ΔortR
0 min
20 min
40 min
60 min
D
Survival Rate (%)
Time (min)
UA159
UA159/pDL278
UA159/pDL278-ortR
UA159 ortR
*
***
E
H_2O_2 (mM)
UA159
UA159/pDL278
UA159/pDL278-ortR
UA159 ΔortR
F
Ratio (Inhibition Zone/Disc Diameter)
H_2O_2 (mM)
UA159
UA159/pDL278
UA159/pDL278-ortR
UA159 ΔortR
***
***

Fig 1